

Synthesis, characterization and application of Lignosulphonate-g-poly(sodium acrylate) hydrogel

Manu, Rajinder K. Gupta* & Devendra Kumar

Department of Applied Chemistry, Delhi Technological University, Delhi, India

*E-mail: rkg67ap@yahoo.com

Received 9 May 2023; accepted 9 September 2023

Natural polymer-based hydrogels are of great interest to research community owing to their inherent characters of environment friendliness and biodegradability. Current work aims to synthesize lignosulphonate grafted sodium acrylate hydrogel (LS-g-SAH) and investigate its application in urea release behaviour. The hydrogel has been characterized by different techniques. The release kinetics has been analyzed by using a UV-visible spectrophotometer. The optimized composition of lignosulphonate, KPS, and N,N'-MBA has shown the highest water absorbency of 560 g g⁻¹ in distilled water. The equilibrium swollen LS-g-SAH 12 hydrogel has slowly released 60% of loaded urea in 24 h and followed first-order release kinetics. Soil treatment with hydrogel has shown a significant effect in reducing the water evaporation rate. It also improved the seed germination and average height of wheatgrass. The synthesized LS-g-SAH is, thus, expected to have potential application in modern sustainable agriculture.

Keywords: Hydrogel, Lignosulphonate, Release kinetics, Sustainable agriculture, Urea release

As world's seventh largest country, India has approximately 157 million hectares of arable land, accounting for 53.2% of the total area. The land is continuously degraded by different means, thus reducing the total production potential to less than 20 percent. Therefore immediate attention is required in upgrading soil fertility, which caused less productivity due to low water retention capability, poor structure, high infiltration rate, low clay and humus content, and loss of agrochemicals through deep percolation or leaching¹.

A super absorbent crosslinked polymer known as hydrogel is a potential material to solve soil-fertility problems. Hydrogel is a 3D network structure composed of chemically or physically crosslinked polymers. It can hold a massive volume of water due to its swollen state's surface tension and capillary forces. The rate of water absorption by hydrogel is affected by the functional group and the density of the crosslinking network². Natural biodegradable polymers should be used to develop economical agricultural water-absorbent materials. Nowadays, researchers are paying great attention to lignocellulosic polymeric material as a favourable, sustainable, and large-scale asset to be used as a chemical component in various syntheses. In this regard, lignin is a renewable feedstock readily

available in an adequate amounts³. Lignin accounts for 16-33% of the biomass and is predominantly present in the secondary cell walls of terrestrial plants⁴. Lignin comprises three types of phenylpropane monomers known as monolignols. These monolignols are a) coniferyl alcohol, b) sinapyl alcohol, and c) p-coumaryl alcohol⁵. This inexpensive waste of pulp manufacturing process is the only scalable renewable raw material that consists of aromatic moieties⁶. It is also easily accessible, affordable, and underutilized today⁷.

Also, a lignin hydrogel based study by Bukhard et al. showed that the synthesized hydrogels could degrade up to 14% in just 60 days as compared with acrylamide-based hydrogels, indicating degradation of just 2% in 120 days⁸. Lignin has antimicrobial, antioxidant, and stabilizer properties⁹. It has also been used for metal elimination. For example, graphene hydrogel based on lignosulphonate, manufactured in a column system, rapidly eliminated Pb²⁺ from the aqueous solution (Thakur et al., 2017). A free-standing lignin-based film with superior electrochemical performance was manufactured by using poly(N-vinyl imidazole)-co-poly(poly(ethylene glycol) methyl ether methacrylate)⁶. However, there has been little exploration of using lignin-based hydrogel for controlled-release applications in

agriculture. Song et al. in 2020 synthesized novel lignin, konjac flour, and sodium alginate hydrogels, which proved to be efficient when tested for the growth of tobacco plants in drought-like conditions. They exhibited high water retention capacity and reduced soil nutrient leaching¹¹. Urea is one of the most commonly used nitrogen fertilizers globally. But due to its leaching losses, its use efficiency is relatively low (on average 30-35%). It is a waste of resources that also results in the pollution of the environment. Slow-release urea through hydrogel is an effective way to address this issue¹². In this work, Lignosulfonate grafted poly(sodium acrylate) hydrogels (LS-g-SAH) have been synthesized and used for agricultural applications. The sample LS-g-SAH 12 was selected for the detailed investigation, and characterized using solid-state ¹³C CP-MAS NMR, scanning electron microscopy (SEM), Fourier-transform infrared (FTIR) spectroscopy, X-ray diffraction (XRD), thermo-gravimetric analysis (TGA) and rheology, and urea release kinetics. Additionally, a control with a composition comparable to LS-g-SAH 12 but lacking lignosulfonate was compared to the synthesized hydrogels.

Experimental Section

Materials

Lignosulfonic acid sodium salt (LS) (Mol wt. ~ 52,000) was purchased from Sigma Aldrich. Acrylic acid (AA) and N,N'-methylenebisacrylamide (N,N'-MBA) were bought from CDH Pvt Ltd. Potassium persulfate (KPS) were purchased from SD fine chem Ltd. Urea and NaOH were purchased from CDH Pvt Ltd, and Qualikems Fine Chem Pvt. Ltd., respectively.

All necessary water-based polymerization solutions were prepared using distilled water.

Synthesis of LS-g-SAH

The free radical co-polymerization technique was used to synthesize LS-g-SAH, where KPS and N,N'-MBA were utilized as an initiator and crosslinker, respectively. At room temperature, NaOH was added to neutralize acrylic acid. The desired amount of LS, AA, NaOH, N,N'-MBA, and KPS was stirred for 2 h continuously. The reaction product was then heated in a water bath preset at 60°C for 2 h. After co-polymerization, the hydrogel was cut into thin slices and immersed in distilled water for 24 h to remove the unreacted chemicals. The hydrogel was then oven-dried at 50°C until constant weight¹³. Fig. 1 Shows the visual representation of the synthesis of LS-g-SAH and Table 1 summarizes the different formulations of synthesized hydrogels.

Characterization of LS-g-SAH

The FTIR spectra in the range of 4000 to 650 cm⁻¹ were recorded using Perkin Elmer 2000 FT-IR spectrometer. The solid-state ¹³C-NMR analysis of samples was done on a Bruker Ascend-400 spectrometer operating at 400 MHz. The surface morphology was determined through SEM on EVO 18 Research, Zeiss, instrument. TGA was conducted on Perkin Elmer, Thermogravimetric Analyzer, TGA 4000 in Nitrogen environment with a uniform heating rate of 10 °C/min. XRD measurements were recorded through RIGAKU with source Cu-Kα performed at a voltage of 50 kV. The rheological analysis was carried out using Anton Par Rheometer (Model: Anton Par, Modular Compact Rheometer,

Table 1 — Various compositions used in synthesis with their swelling index

Formulation	LS (g)	NaOH (mol/L)	AAA (mL)	KPS (g)	NN-MBA (g)	Swelling index (g/g)	Gel %
LS-g-SAH 1	0.1	8.07	7.1	0.1	0.05	190.3	62.11
LS-g-SAH 2	0.1	8.07	7.1	0.1	0.07	172.82	63.38
LS-g-SAH 3	0.1	8.07	7.1	0.1	0.1	111.6	73.26
LS-g-SAH 4	0.1	8.07	7.1	0.1	0.12	60.22	77.59
LS-g-SAH 5	0.1	8.07	7.1	0.1	0.15	39.68	92.16
LS-g-SAH 7	0.1	8.07	7.1	0.04	0.08	89.31	85.31
LS-g-SAH 8	0.1	8.07	7.1	0.05	0.08	172.92	92.73
LS-g-SAH 9	0.1	8.07	7.1	0.08	0.08	252.83	96.90
LS-g-SAH 10	0.1	8.07	7.1	0.12	0.08	120.92	92.50
LS-g-SAH 11	0.1	8.07	7.1	0.14	0.05	560.24	95.28
LS-g-SAH 12	0.2	8.07	7.1	0.14	0.05	397.22	91.20
LS-g-SAH 13	0.3	8.07	7.1	0.14	0.05	336.35	85.99
LS-g-SAH 14	0.4	8.07	7.1	0.14	0.05	320.63	75.33
LS-g-SAH 15	0.05	8.07	7.1	0.14	0.05	248.32	72.04
LS-g-SAH 16	0.08	8.07	7.1	0.14	0.05	461	89.36

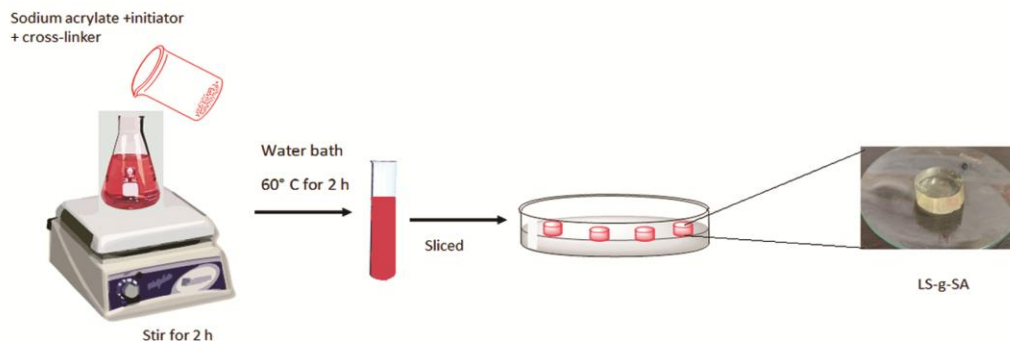


Fig. 1 — Visual representation of the synthesis of LS-g-SAH

MCR 302) with PP-25 parallel plate and 2.5 mm inter-platen gap.

Swelling experiment

The swelling studies for LS-g-AA hydrogels were performed in pH 4.0, 7.0, and 9.2 buffer and distilled water at 37°C. Dried hydrogel discs were weighed and placed in various pH media. These were removed after a fixed time interval and weighed. Filter paper has been used to remove additional surface water¹⁴. The samples were observed in triplicate. The swelling index (SI) (g g^{-1}) was calculated using the given Eq. (1):

$$SI = \frac{M_1 - M_2}{M_2} \quad \dots (1)$$

Where, M_1 and M_2 represent the weight of equilibrium swollen hydrogel discs and wt. of dried hydrogel discs, respectively.

Gel content determination

The fraction of insoluble weight is known as gel content. The soluble part of the gel is extracted using the Soxhlet apparatus in boiling water for 24 h to obtain the gel content. The swollen hydrogels were removed from the apparatus and oven dried at 50°C¹⁴. The gel content of hydrogel was determined from Eq. 2.

$$\text{Gel content (\%)} = SI = \frac{M_g}{M_i} * 100 \quad \dots (2)$$

Where, M_e and M_i are the respective weights of dry hydrogel before and after extraction.

Measurement of the highest water-retention capacity (WH%) of LS-g-SAH treated soil

This study was carried out using the garden soil of DTU, Delhi. Up to 1% of the hydrogel was added to 50 g of dry soil (less than 30 mesh size) and placed in

a PVC tube (4.5 cm diameter). Its bottom was secured with a nylon cloth and weighed to obtain W_1 . The treated soil samples were slowly saturated by adding tap water until they started to seep out from the bottom. The tubes were then re-weighed and marked W_2 . A control experiment without LS-g-SAH was also conducted¹⁵. The largest water-retention capacity of treated soil was determined using Eq. 3.

$$\text{WH\%} = \frac{W_2 - W_1}{50} * 100 \quad \dots (3)$$

Water Evaporation rate of LS-g-SAH and soil

A water evaporation test was used to investigate LS-g-SAH-treated soil's ability to retain water within its system structure for 55 days. Oven-dried soil (at 60°C for 48 h) was used to prepare different sets of hydrogel-treated soil along with a control set. Each mixture was fed with 50 mL distilled water and weighed (marked as M_i). The total water, soil, and hydrogel weight was kept as ' M_T .' Then, these were placed at room temperature and weighed daily (M_t)¹⁶. Here, the effect of LS-g-SAH in different amounts on soil was studied by considering the water evaporation loss value from blank soil as a control. The water evaporation ratio (WER) was determined using Eq. 4.

$$\text{WER} = \frac{M_i - M_t}{M_T} * 100 \quad \dots (4)$$

Loading and release of urea by LS-g-SAH

Urea was loaded onto the hydrogel by immersing a pre-weighed dry LS-g-SAH into a urea solution (0.034 mol/L) for 24 h. After that, the swollen gels were removed from the water and dried till a constant weight was achieved.

The amount of urea released by LS-g-SAH was evaluated by soaking the dried urea-loaded samples in

a beaker with 100 mL of distilled water at ambient temperature. Later, 1 mL water was drawn from the medium at fixed intervals to observe the released urea, and the same amount of distilled water was added to the beaker to keep the volume constant¹⁷.

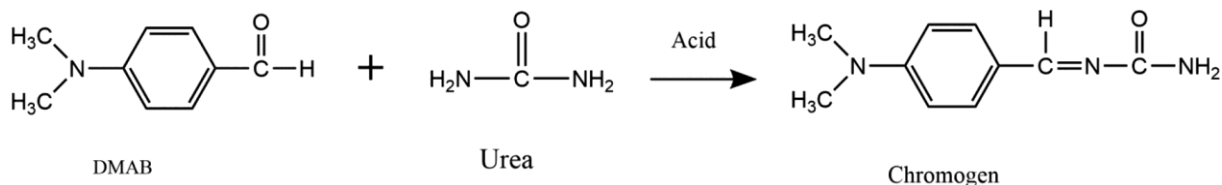
A standard method from “The Specialized Standard of the People’s Republic of China (SN/T 1004-2001)” was used to determine the concentration of urea residue. At 430 nm, a spectrophotometer detected a complex compound of urea and p-dimethylamino benzaldehyde (DMAB). The general reaction showing the formation of chromogen that follows Beer-Lambert law and absorbs energy at 430 nm in the UV-visible spectrum is shown below in Scheme 1. Then, the standard calibration curve was used to formulate the below-mentioned formula for the determination of urea concentration¹².

$$C \text{ (ppm)} = \frac{A-0.1735}{0.0002} \quad \dots (5)$$

Where, A is the UV absorbance of solution of unknown concentration.

Plant Growth Performance study

Three sets of 300 g of soil were placed in plastic pots with filter paper placed below with a small hole; (a) only urea, (b) control hydrogel-loaded urea, and (c) LS-g-SAH loaded with urea (at a depth of 5 cm). A plastic pot with direct urea in soil without hydrogel was kept as a check. Fifteen wheat seeds were sown in all three plastic pots with the same amount of hydrogel. Pots were exposed to environmental conditions, and irrigation was kept constant from day one for all containers. Growth profiles for all wheat grasses were observed at various time intervals. Germination was recorded by counting germinated seeds over two weeks. Just the appearance of the radicle was considered an indicator of seed germination. The plant shoots and roots were removed carefully from the soil. The shoot and root lengths and their fresh weight were recorded. The plant material was dried for 24 h at 70°C to determine the dry mass¹⁸.



Scheme 1 — DMAB-urea reaction

Results and Discussion

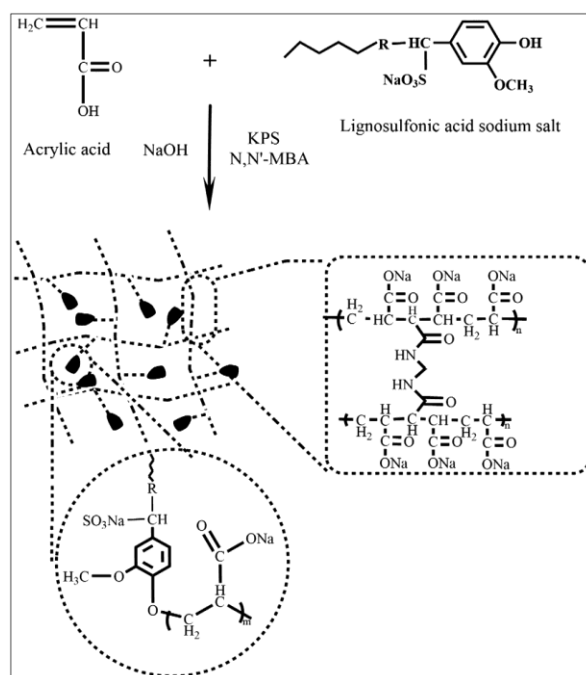
Mechanism of the formation of lignosulfonate-g-sodium acrylate hydrogels

The KPS used as an initiator generated anion radicals which further helped to generate phenoxy radicals on LS. The active radicals also reacted with the vinyl groups of sodium acrylate, leading to the propagation of chain-forming poly sodium acrylate. This poly(sodium acrylate) propagated until crosslinked and terminated by MBA to form lignosulfonate-g-acrylic acid hydrogels, as shown in Scheme 2. The electrostatic repulsion created by the negatively charged carboxylate ions in the poly(sodium acrylate) polymer chains will lead to a network expansion. This will improve the hydrogel’s capacity to absorb water¹⁵.

Characterization of hydrogel

Fourier-transform infrared (FTIR) spectroscopy

The IR spectra of LS, ctrl, and LS-g-SAH are shown in Fig. 2. The -OH stretching vibration of LS is observed as a broad band around 3,303 cm⁻¹. LS, ctrl



Scheme 2 — Synthesis of LS-g-SAH

and LS-g-SAH show a band around $2,920\text{ cm}^{-1}$ due to C–H stretching in $-\text{CH}_2$ or $-\text{CH}_3$ groups. The vibration of the aromatic skeleton is observed from the two firm peaks at $1,572$ and $1,417\text{ cm}^{-1}$.⁴ The strong peak at $1,046\text{ cm}^{-1}$ arises due to C–O–S stretching vibration, and the peak at $1,114\text{ cm}^{-1}$ is assigned to O=S=O antisymmetric stretching vibration in the LS.⁴ Both these characteristic peaks confirm the presence of LS in LS-g-SAH. Further, new peaks were found when LS was compared to LS-g-SAH. The strong bands at 1404 and 1554 cm^{-1} are

due to the asymmetric stretching in the carboxylate anion. The broad band and a peak at 1317 cm^{-1} and 627 cm^{-1} , respectively, correspond to the C–N and O=C–N groups of N,N'-MBA¹⁹.

SS ^{13}C CP-MAS

Solid state ^{13}C NMR spectroscopy is a powerful tool for the structural characterization of polymers. The spectra of LS, LS-g-SAH, and ctrl hydrogel prepared by graft co-polymerization are presented in Fig. 3. Peaks around 45 ppm and 185 ppm of LS-g-SAH and ctrl were assigned to saturated aliphatic chains and C from

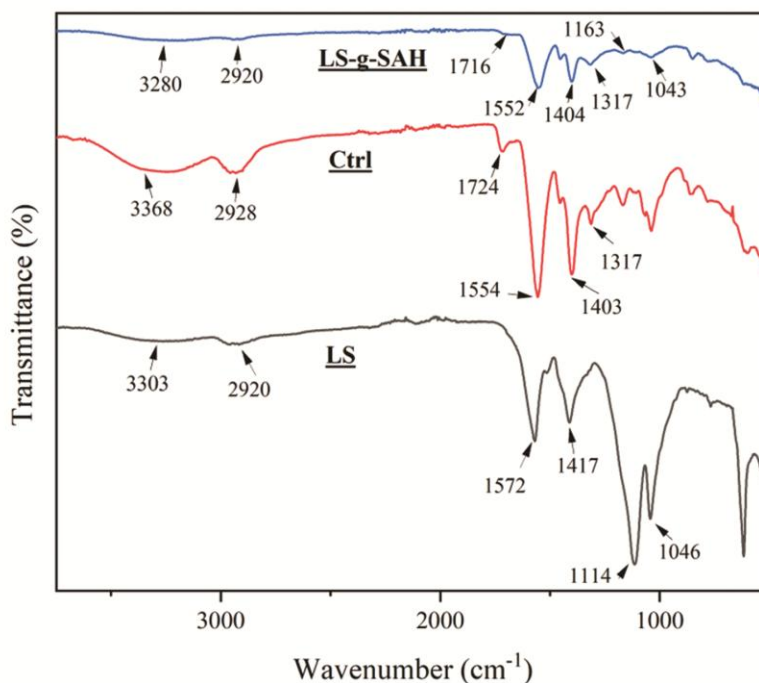


Fig. 2 — FTIR spectra of (a) LS, (b) Ctrl and (c) LS-g-SAH

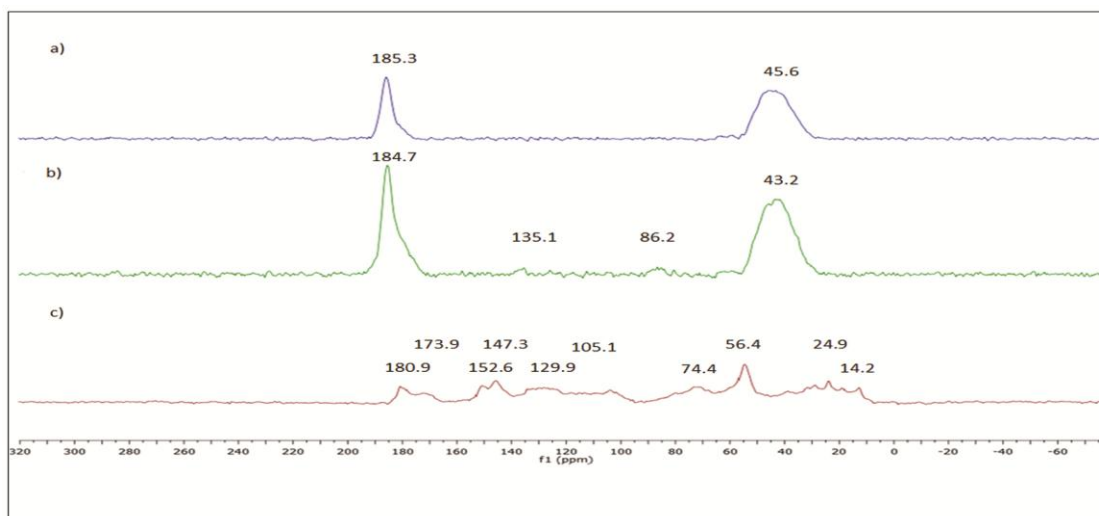


Fig. 3 — SS ^{13}C CP-MAS NMR spectrum of (a) ctrl, (b) LS-g-SAH, and (c) sodium LS

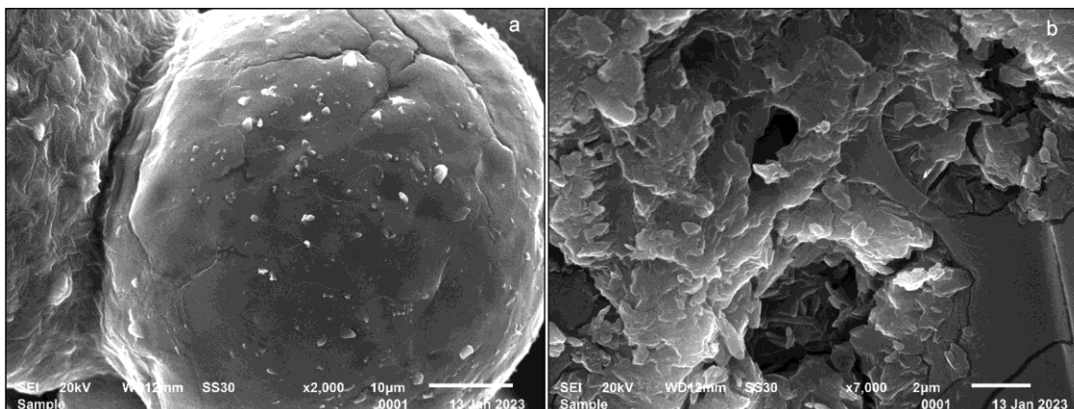


Fig. 4 — The SEM images of (a) LS and (b) LS-g-SAH

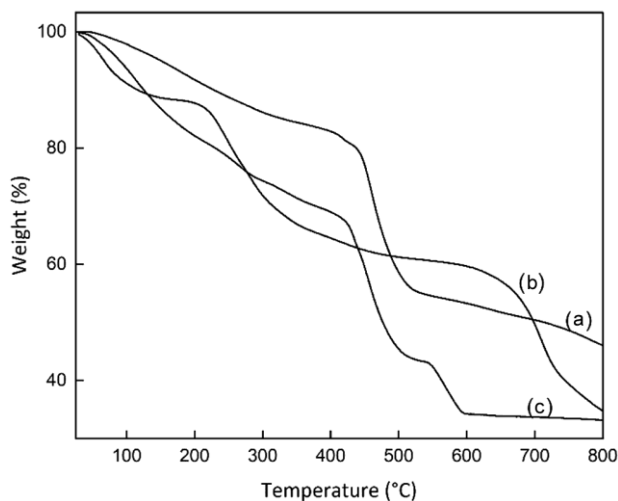


Fig. 5 — TGA plots of (a)-LS-g-SAH, (b) LS and (c) Ctrl

carbonyl ester (COONa), COOH, respectively. Characteristic peaks of basic aromatic and aromatic rings with branched C-C bonds can be observed in the range of 140-110 ppm and 75-10 ppm. The appearance of signals around 50-10 ppm in LS represents aliphatic C chain²⁰⁻²³. Most of the peaks of LS merged inside LS-g-SAH due to their low intensity. However, the presence of peaks at 135.1 ppm and 86.2 ppm confirms the presence of LS in LS-g-SAH. The results support the observations of the FT-IR spectra. The presence of free COOH groups and crosslinks probably increased the intensity of the peak at 184.7 ppm.

Scanning electron microscopy (SEM)

The SEM images of the LS and LS-g-SAH samples at the different magnifications are presented in Fig. 4. The surface of LS is even and smooth in granular form. On the contrary, the LS-g-SAH is rough, uneven, and porous. This could be due to the grafting of LS onto poly(acrylate) chain, further facilitating the adsorption of more water.

Thermal analysis

As shown in the thermograms (Fig. 5) of both LS and LS-g-SAH samples three weight loss ranges have been observed in the range of 29-802°C. The initial 16.3% weight loss at the stage (70-380°C) in LS-g-SAH is due to moisture loss from the polymer. Between 436-514°C, the weight loss percent of 23.4 is mainly due to the beginning of decomposition. The third stage, from 660-781°C, is the decomposition of the main polymeric backbone with a weight loss of 19.7%⁶. For LS, up to 150°C, the first decomposition is associated with removing volatile compounds and moisture, like acetaldehyde, acetone, and methanol. With the increase in temperature from 150°C to 250°C, LS began to decompose, known as vitrification transformation. The primary decomposition occurred between 200 and 400°C. Weight loss of LS above 500°C could be attributed to the CO from degrading C=O, C-O-C, and degeneration of aromatic rings^{24,25}. The results from ¹³C NMR and LS FTIR also support high amounts of C=O groups. Moreover, LS likely reacted with carbon from a sodium-containing salt that served as an activator for the dry pyrolysis process, further creating a mass loss between 650 and 800°C²⁶. The point of the highest rate change is found at approximately 500°C for LS-g-SAH, 450°C, and 270°C for ctrl and LS, respectively. LS-g-SAH had a higher residual weight of about 83% up to 400°C compared to 69% and 64% of ctrl and LS. Similarly, at 800°C, the LS-g-SAH resulted in more than 46% of residual mass when compared to just 34% and 33% of the residual mass of LS and ctrl hydrogels. This observation indicated that grafting of LS has improved the thermal stability of LS-g-SAH.

X-ray diffraction

The XRD patterns observed in the 2θ range of 20°-80° of lignin showed several peaks at 23.12°,

25.52°, 27.32°, 28.34°, 31.64°, 33.60°, 40.48°, 45.34°, 56.36° and 75.16° (Fig. 6). The LS-g-SAH and ctrl showed two broad complex peaks in the range with their maxima at 22° and 32°. The observed maxima are characteristic of an amorphous polymer structure²⁷. The data revealed that lignin's crystallinity is destroyed after grafting onto poly(sodium acrylate). Such a similar result has been observed by grafting carboxymethyl cellulose on sodium acrylate²⁸.

Rheology

The knowledge of rheology can easily explain the relationship between chemical structure and the macroscopic behaviour of hydrogels²⁹. Rheological properties of LS-g-SAH are compared with ctrl to investigate the effect of the presence of lignin in the hydrogel, as shown in Fig. 7. During the amplitude sweep test, the shear stress amplitude was changed at a rate of 10 rad/s. At low deformation, the loss modulus (G'') and storage modulus (G') are consistent, indicating that the hydrogel structure remained unaffected. It is called a linear-viscoelastic region (LVE). The disruption of structure with decreased modulus suggests the termination of the LVE region. The ctrl and LS-g-SAH showed viscoelastic solid behaviour up to a high strain of 402 and 511%, representing that LS-g-SAH may bear a higher shear strain than ctrl.

The frequency varied from 0.1 to 500 rad/s during the frequency sweep test while keeping the shear strain % within the LVE region constant. It was observed that the loss modulus was found to be prevalent at higher frequencies while the storage modulus was prevalent at lower frequencies representing the viscoelastic solid behaviour. $\tan \theta$

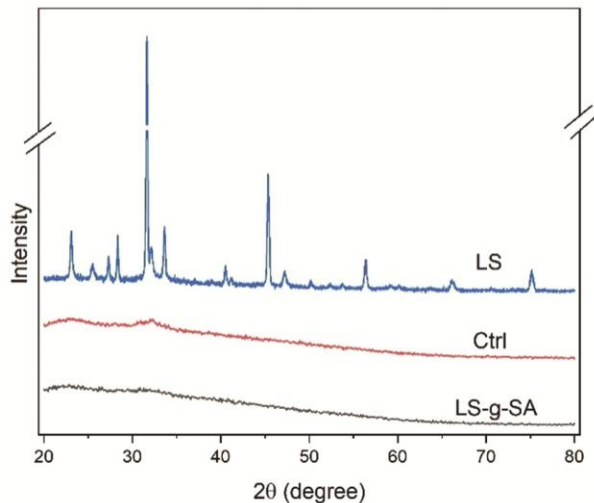


Fig. 6 — XRD plots of LS, Ctrl, and LS-g-SAH

(dimensionless) generally varies from 0 to 1 for viscoelastic solutions. For an ideal viscous behaviour, $\tan \theta$ is infinity, i.e., θ is 90° and for a perfect elastic behaviour, $\tan \theta$ is 0, i.e., θ is 0°.³⁰

It was observed from Table 2 that the cross-over point for LS-g-SAH falls in the low-frequency region (126 rad/s), indicating that its chain-chain interaction breaks at a lower frequency in comparison to ctrl. LS-g-SAH and ctrl had a loss factor of 0.04 and 0.018, representing the dominance of elastic behavior at low frequency and viscous behavior at high frequency, which agrees with the previously reported literature³¹. However, ctrl hydrogel shows more elastic behaviour

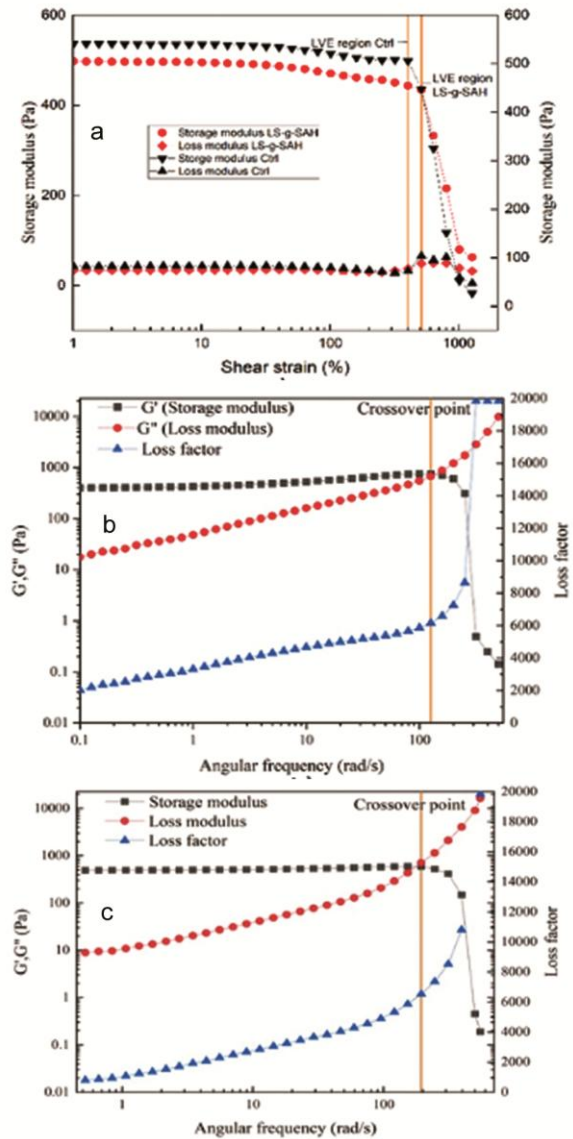


Fig. 7 — Rheological analysis: (a) amplitude sweep, (b) Frequency sweep of LS-g-SAH and (c) Frequency sweep of Ctrl hydrogel

Sample	Low frequency		Loss factor Tan θ	Cross-over point Angular frequency (rad/s)	High frequency		
	Storage modulus G' (Pa)	Loss modulus G'' (Pa)			Storage modulus G' (Pa)	Loss modulus G'' (Pa)	Loss factor Tan θ
LS-g-SAH	400	17.58	0.04	126	0.14	1722	infinite
Ctrl	491	8.89	0.018	194	0.19	2107	infinite

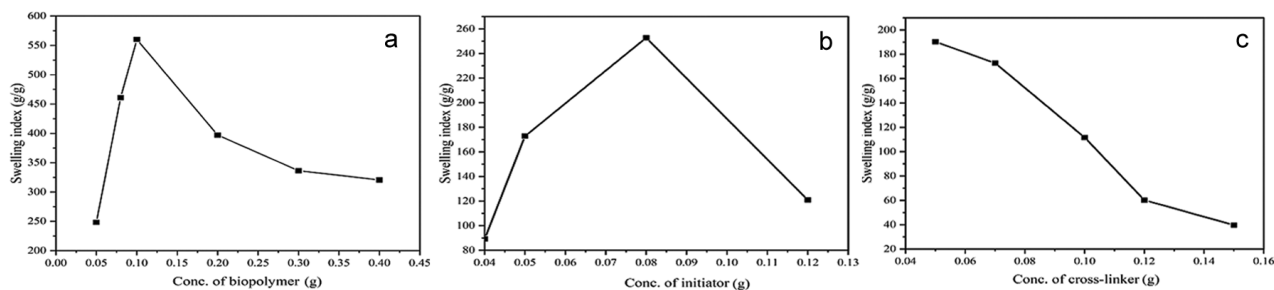


Fig. 8 — Effect of variation of (a) biopolymer, (b) initiator and (c) crosslinker on the swelling index

at low frequencies. Frequency sweep data of LS-g-SAH and ctrl hydrogels are shown in Table 2.

Gel content (%)

The gel content percentage of LS-g-SAH present in Table 1 was calculated using Eq.(2). The gel percentage of hydrogels varied according to the concentration of crosslinker, biopolymer, and initiator. The gel content reduced as the concentration of the crosslinker and biopolymer increased. In contrast, the initiator initially enhanced the gel content but decreased when added in amounts greater than 0.08 g. Gel contents of synthesized hydrogels were found in the 64 - 97 % range.

Effect of variation of framework parameters on the swelling index

The relationship between framework parameters and water absorbency was investigated by Flory, who concluded that hydrogel absorption depends on several parameters³². Therefore, the variables affecting the reaction, such as the concentration of biopolymer, initiator and crosslinker are studied to obtain the optimum reaction conditions.

Effect of biopolymer

The concentration of hydrophilic biopolymer is one of the influencing factors of the swelling property of hydrogel. Fig. 8(a) shows that LS was varied from 0.05 g to 0.4 g in hydrogel to find the optimum concentration. Adding LS provided a more significant number of diverse hydrophilic groups to the hydrogel, resulting in an increment in the SI. After the LS

content reached 0.1 g, the amount of ionic hydrophilic groups in the hydrogel, such as sulfonic acid and carboxyl groups, could have become higher than the non-ionic hydrophilic groups such as amide group and hydroxyl group, which further led to the declination of the SI.³³

Effect of initiator

The reaction initiator creates active sites on the polymer. Thus, it plays a crucial role in the preparation of hydrogel. The SI of hydrogel increased with an increase in initiator concentration from 0.04 g to 0.08 g. Afterward, it decreased with the increasing amount of the initiator, according to Fig. 8(b). The maximum water absorbance was obtained at 0.08 g of the initiator. An increase in the amount of initiator up to 0.08 g generated more free radicals, resulting in larger chain ends in the network while shortening the average length of the kinetic chain. Accordingly, the SI would increase. However, an initiator concentration greater than 0.08 g may have increased the reaction velocity and decreased the network space of the polymer, which resulted in a decrease in the SI.³⁴

Effect of concentration of crosslinker

It is evident from Fig. 8(c) that the SI sharply decreased with the increase in the crosslinker concentration of hydrogel. The graft reaction did not occur effectively with a concentration of MBA lower than 0.03 g resulting in a jelly-like product with poor dimensional stability. Beyond this amount, adding

more crosslinker to hydrogel resulted in more crosslink junctions in the polymeric chains. It increases the extent of crosslinking and reduces the free available volume inside the polymeric network^{34,35}. This results in a less swelling tendency of the hydrogel.

Swelling studies

In general, the swelling index of different formulations in distilled water has been reported in Table 1. The swelling performance of L10 was investigated in various pH, i.e., pH 4.0, 7.0, and 9.2, and distilled water. Fig. 9 shows the enhancement in equilibrium SI from 51 to 73 with an increase in pH from 4, 7, and 9.2. Lower swelling of hydrogel in an acidic medium may be attributed to the improper ionization of the crosslinked network. Hence, at a lower pH, a collapsed state was observed. However, in alkaline conditions, electrostatic repulsions may have been produced by the carboxylate anions (COO⁻). This might have caused a widening of space present in hydrogel networks, leading to an increase in the SI of the hydrogel^{35,36}.

Agricultural applications of LS-g-SAH

Highest water retention capacity

Water availability in the soil is of utmost importance for better plant growth. As a result, the impact of LS-g-SA hydrogel on soil's maximum water retention capacity (WH%) was investigated. The amount of absorbed water and the corresponding concentration of incorporated hydrogel is shown in Fig. 10. It proved that the synthesized hydrogel exhibited excellent water-absorbing capacity and could be used to improve the soil water-retention

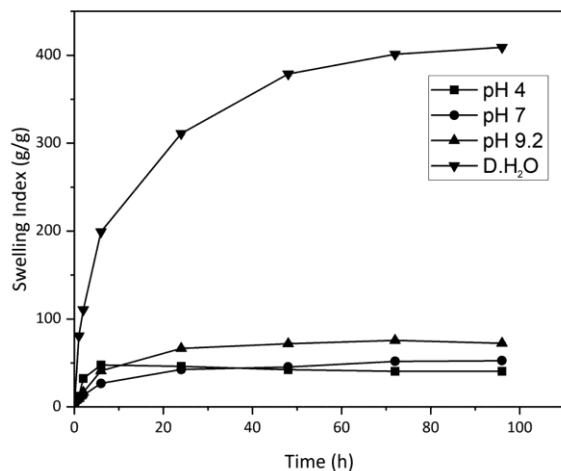


Fig. 9 — Swelling study of hydrogel

capacity and reduce the frequent irrigation requirement.

Evaporation study

Evaporation refers to the water loss from the soil directly to the atmosphere through water vapour. The water-holding capacity of soil affects the water evaporation rate of the soil. The control's water evaporation ratio from the study was higher than soil amended with LS-g-SAH, probably due to the interaction between water and polymer molecules and the macromolecular network hindrance¹⁶. Fig. 11 shows that adding just 0.6 g LS-g-SAH to the soil reduced the evaporation rate from 99 to 76.69% of the total added water on the 54th day.

Release kinetics of urea

The power of law equation is used to understand the mechanism involved in releasing urea.

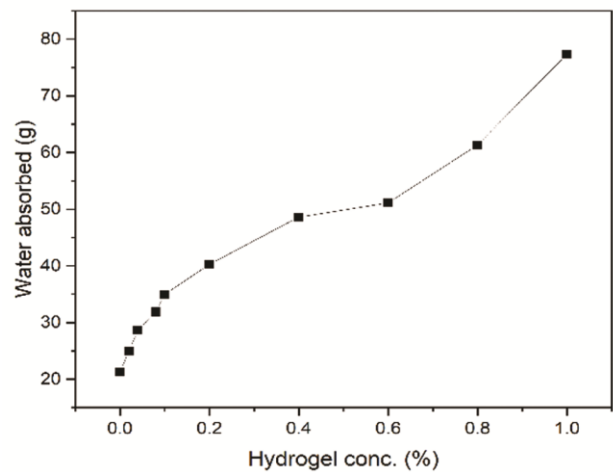


Fig. 10 — Water retention capacity plot of soil amended with LS-g-SAH

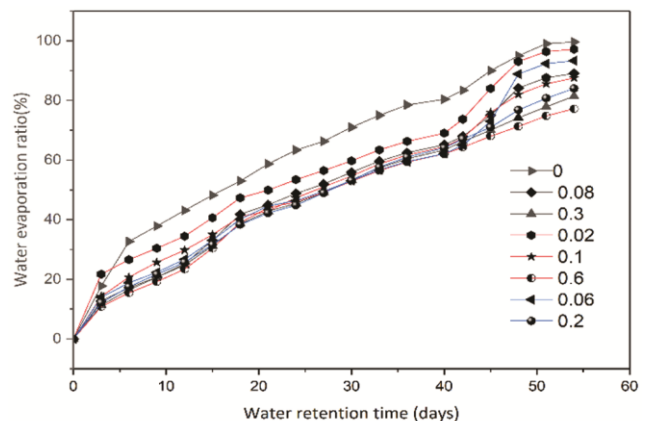


Fig. 11 — Water evaporation study of soil amended with different concentrations of LS-g-SAH

$$\frac{M_t}{M_\infty} = k_{kP} t^n \quad \dots (6)$$

where M_t and M_∞ Represents the urea released at time t and the equilibrium point, respectively. Whereas the ratio of M_t to M_∞ denotes the fraction of total urea released at the time ' t ', while ' k ' is a polymer structure constant. The coefficient ' n ' describes the type of diffusion involved. Only the section of the release curve where the ratio $\frac{M_t}{M_\infty} < 0.6$ should be used to determine the exponent ' n '^{37,38}.

Diffusion-controlled release is indicated by a Fickian diffusion mechanism with $n \geq 0.45$, whereas $0.45 < n < 0.89$ corresponds to non-Fickian transport, and $n = 0.89$ corresponds to case-II relaxational transport, which specifies swelling-controlled release³⁸.

Urea release kinetics studied using different models such as a) first order, b) Korsmeyer–Peppas, c) Higuchi model in distilled water are shown in Fig. 12, The slow-release process of urea through LS-g-SAH occurs in the following manner; firstly, the water tries to enter the hydrogel. Afterward, the hydrogel starts to swell by absorbing water until a dynamic exchange

is developed between the free water of the hydrogel and the water present in the soil. Meanwhile, the urea in the hydrogel matrix continues to dissolve and diffuse. It gets released into the water due to the osmosis differences and dynamic exchange of free water¹⁶.

From Table 3, " n " is 0.8193, representing a non-Fickian diffusional release of urea from the synthesized hydrogel. The coefficient of determination values (R^2) showed its maximum value to be 0.9932 for the first-order kinetics; hence, the release followed the First order kinetics model.

Plant Growth Performance

The plant growth performance study using the LS-g-SAH is shown in Fig. 13. The wheatgrass growth can be observed by the changed total dry and fresh weight, the average number of germinated seeds, the average wheatgrass height, and the average shoot height of all samples. All these are mentioned in Table 4. The height of the plants increased with the advancing age of the crops. On the 14th day, significantly tallest grasses (the tallest grass was 27 cm) were recorded in LS-g-SAH, followed by sample B, i.e., ctrl, though the shortest plants were recorded

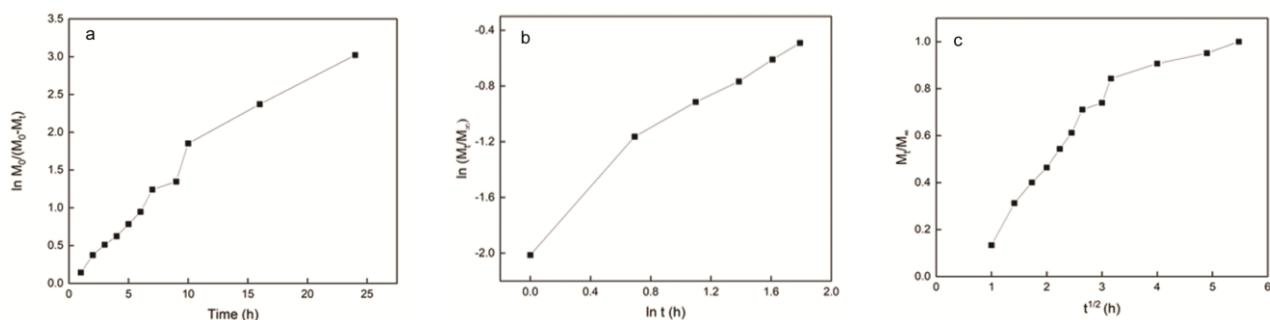


Fig. 12 — Urea release kinetics using (a) first order, (b) Korsmeyer–Peppas and (c) Higuchi model in distilled water

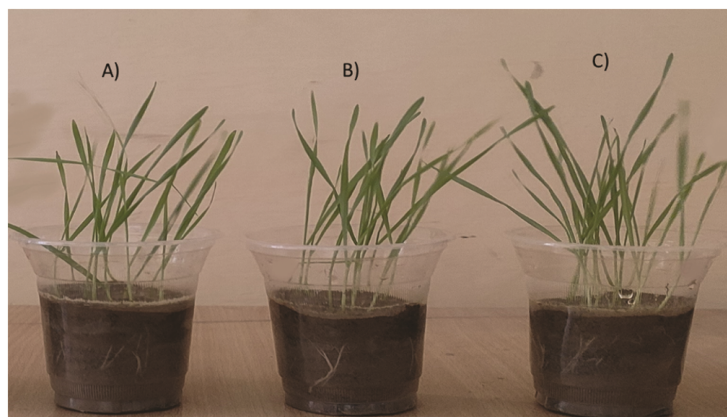


Fig. 13 — Effect of hydrogel treatment on wheatgrass after 14 days using (A) only urea, (B) control hydrogel-loaded urea, and (C) LS-g-SAH loaded with urea

Table 3 — Mathematical models used for the study of release kinetics from LS-g-SAH

Model	Equation	Parameter		R sq.
First-Order	$f = 100[1 - e^{-k_1 t}]$ f = amount of the released drug k ₁ = rate constant, t = time	k ₁	0.174	0.9932
Higuchi	$f = k_H t^{0.5}$ f = amount of the released drug k _H = Higuchi dissolution constant t = time	k _H	22.134	0.8242
Korsmeyer–Peppas	$f = k_{KP} t^n$ k _{KP} = constant depicting the experimental parameters f = amount of the drug released n = release exponent	k _{KP} n	0.4099 0.8193	0.9656

Table 4 — Wheatgrass growth parameters on the 14th day: (A) only urea, (B) control hydrogel-loaded urea, and (C) LS-g-SAH loaded with urea

Sample	Total fresh weight of wheatgrass (Average) (g)	Total dry Weight of wheatgrass (Average) (g)	Average number of germinated seeds (per pot) at 14 th day	Average wheatgrass height (cm) at 14 th day	Average shoot height (cm) on the 14 th day
A	0.7927	0.2860	13	17.2	12.4
B	0.8102	0.3002	12	17.7	12.8
C	0.8993	0.3004	15	19.7	14.4

under sample A. The germination and growth of seeds are known to be improved with the prolonged availability of urea. LS-g-SAH showed 100% germination followed by control hydrogel (86.6%), i.e., sample B and untreated soil (80%) urea release, respectively.

Conclusion

Novel LS-g-SAH was synthesized and loaded with urea using the gravitational equilibrium method. When observed in different media, the maximum water absorbency was 560 g/g in distilled water. Using synthesized hydrogel remarkably raised the soil's water-holding capacity from 21.27 to 77.3 g. Also, the water evaporation rate reduced from 99 to 76.69% of the total added water. The release kinetics study of urea in water revealed that LS-g-SAH showed a slow-release pattern with 60% release in 24 h following first-order release kinetics. The release pattern followed the Non-Fickian release mechanism. The increased height of wheatgrass also confirmed the beneficial effects of LS-g-SAH. Thus, the synthesized poly(sodium acrylate) hydrogel based on lignin can serve as a water retention agent and has the potential to be used for the gradual release of various agrochemicals.

Acknowledgment

The authors would like to acknowledge the financial support of the Department of Applied Chemistry, Delhi Technological University, Delhi.

References

- Rajakumar R & Sankar J, *Int J Appl Pure Sci Agric*, 2 (2016) 163.
- Wang Q, Guo J, Lu X, Ma X, Cao S, Pan X & Ni Y, *Int J Biol Macromol*, 181 (2021) 45.
- Mandlekar N, Cayla A, Rault F, Giraud S, Salaün F, Malucelli G & Guan J P, *Lignin - Trends Applications In Tech*, (2018).
- Yu C, Wang F, Zhang C, Fu S & Lucia L A, *React Funct Polym*, 106 (2016) 137.
- Ludmila H, Michal J, Andrea Š & Aleš H, *Wood Res*, 60 (2015) 973.
- Meng Y, Lu J, Cheng Y, Li Q & Wang H, *Int J Biol Macromol*, 135 (2019) 1006.
- Fernández-Pérez M, Flores-Céspedes F, Daza-Fernández I, Vidal-Peña F & Villafranca-Sánchez M, *Ind Eng Chem Res*, 53 (2014) 13557.
- Wilske B, Bai M, Lindenstruth B, Bach M, Rezaie Z, Frede H G & Breuer L, *Environ Sci Pollut Res*, 21 (2014) 9453.
- Thakur V K & Thakur M K, *Int J Biol Macromol*, 72 (2015) 834.
- Thakur S, Govender P P, Mamo M A, Tamulevicius S, Mishra Y K & Thakur V K, *Vacuum*, 146 (2017) 342.
- Song B, Liang H, Sun R, Peng P, Jiang Y & She D, *Int J Biol Macromol*, 144 (2020) 219.
- Zheng T, Liang Y, Ye S & He Z, *Biosyst Eng*, 102 (2009) 44.
- Gupta A P & Warkar S G, *Int J Pharm Bio Sci*, 6 (2015) 516.
- Akalin G O & Pulat M, *J Polym Res*, 27 (2020) 1.
- Ni B, Liu M & Lü S, *Chem Eng J*, 155 (2009) 892.
- Rabat N E, Hashim S & Majid R A, *Procedia Eng*, 148 (2016) 201.
- Raafat A I, Eid M & El-Arnaouty M B, *Nucl Instrum Methods Phys Res Sect B Beam Interact Mater Atoms*, 283 (2012) 71.

- 18 Akhter J, Mahmood K, Mali K A, Mardan A & Ahmad M, *Plant Soil Environ*, 10 (2004) 463.
- 19 Reddy V & Rao R, *Indian J Pure Appl Phys*, 46 (2008) 611.
- 20 Sun Y, Ma Y, Fang G, Li S & Fu Y, *Bioresour J*, 11 (2016) 5731.
- 21 Ma Y, Sun Y, Fu Y, Fang G, Yan X & Guo Z, *Chemosphere*, 163 (2016) 610.
- 22 Tomar R S, Gupta I, Singhal R & Nagpal A K, *Polym Plast Technol Eng*, 46 (2007) 481.
- 23 Mali K K, Dhawale S C & Dias R J, *Int J Biol Macromol*, 105 (2017) 463.
- 24 He M K, He Y L, Li Z Q, Zhao L N, Zhang S Q, Liu H M & Qin Z, *Int J Biol Macromol*, 209 (2022) 258.
- 25 Hemmilä V, Hosseinpourpia R, Adamopoulos S & Eceiza A, *Waste Biomass Valori*, 11 (2020) 5835.
- 26 Zhang J, Zhao L, Yu F & Zang L, *Energy Fuels*, 33 (2019) 8812.
- 27 Adnadjevic B & Jovanovic J, *J Appl Polym Sci*, 107 (2008) 3579.
- 28 Kumar B, Priyadarshi R, Sauraj, Deeba F, Kulshreshtha A, Gaikwad K K, Kim J, Kumar A & Negi Y S, *Gels*, 6 (2020) 49.
- 29 Stojkov G, Niyazov Z, Picchioni F & Bose R K, *Gels*, 7 (2020) 255.
- 30 Yadav R & Purwar R, *Polym Test*, 93 (2021) 106916.
- 31 Sani M I, Teo Y Y & Misran M, *Polym Bull*, 78 (2021) 3399.
- 32 Flory P J, *Principles Polymer Chemistry*, Cornell University Press, Ithaca, NY, (1953) 5.
- 33 Wang X, Wang Y, He S, Hou H & Hao C, *Ultrason Sonochem*, 40 (2018) 221.
- 34 Li W, Wang J, Zou L & Zhu S, *J Polym Res*, 15 (2008) 435.
- 35 Khushbu, Warkar S G & Kumar A, *Polymer*, 182 (2019) 121823.
- 36 Singh B & Sharma V, *Polymer*, 91 (2016) 50.
- 37 Costa P & Sousa L J M, *Drug Dev Ind Pharm*, 29 (2003) 89.
- 38 Alam M A, Takafuji M & Ihara H, *Polym J*, 46 (2014) 293.